AN EFFICIENT NUMERICAL INTEGRATION ALGORITHM FOR THE SINGLE MODE COMPRESSIBLE LEONOV MODEL – COMPLAS XI

M. MIRKHALAF[*], F. PIRES[†] AND R. SIMÕES[†]

[*] Department of Mechanical Engineering (DEMec)
Faculty of Engineering
University of Porto, Porto, Portugal
email: mohsen.mirkhalaf@fe.up.pt

[†] Department of Mechanical Engineering (DEMec)
Faculty of Engineering
University of Porto, Porto, Portugal
email: fpires@fe.up.pt

[†] Institute for Polymers and Composites - IPC / I3N,
University of Minho, 4800-058 Guimarães, Portugal
email: rsimoes@dep.uminho.pt

Key words: Numerical integration, Leonov model, Return mapping.

Abstract. In this contribution, an algorithm for numerical integration of the Leonov elasto-viscoplastic model is proposed. The operator split methodology and the Newton-Raphson method are used to derive the state update algorithm and obtain the numerical solution of the discretized evolution equations. Particular effort is devoted to the reduction of the number of required residual equations in order to have a more efficient numerical implementation. The consistent tangent module is expressed in a closed form as a result of the exact linearization of the discretized evolution equations. The performance of the algorithm is validated through comparison with existing experimental data.

1 INTRODUCTION

As polymeric based materials can have a considerable role in structural applications, it is important to understand how their mechanical performance is affected by the molecular structure, the processing conditions and the geometry of the micro constituents. In order to have an optimal design, optimization of all aforementioned parameters would be highly desireable. Such an optimization would be impossible using only experiments. Consequently, other methods should be used for that goal.

During the last few decades, many researchers have devoted their work to the development of constitutive models for different materials such as metals and polymers. Among others, Haward and Tackray [6] developed one of the earliest one dimensional constitutive models to

predict the behavior of polymeric materials. The model takes into account the strain rate dependency of the yield point and strain hardening. The three dimensional version of Haward and Tackray model was proposed by Boyce et al. [2]. A modified version of this model was later formulated by Wu and van der Giessen [13]. The other constitutive model which is able to predict the typical deformation behavior of polymeric materials is the generalised compressible Leonov model, which has been proposed by Baaijens [1] and extended by Tervoort et al. [9] and Govaert et al. [5].

In order to analyze real problems, an efficient numerical integration algorithm of the constitutive relations, within the finite element framework, is necessary. Since the numerical treatment of the Leonov constitutive relations has not been, to the authors' knowledge, presented in the open literature, an attempt is made to introduce an efficient numerical integration algorithm for the model. Therefore, in the next section, the constitutive relations of the Leonov model are presented. Section 3 deals with the numerical treatment of the constitutive relations. In the subsequent section, two numerical examples and their corresponding results are provided. Finally and based on the obtained results, section 5 presents some conclusions made from this work.

2 CONSTITUTIVE RELATIONS

In this section, the constitutive relations of the Leonov model, used in this work, are presented. In the Leonov model, the total stress is composed of driving and hardening stresses.

$$\boldsymbol{\sigma}^{total} = \boldsymbol{\sigma}^{hardening} + \boldsymbol{\sigma}^{driving} \tag{1}$$

The hardening stress is computed by the following relation:

$$\boldsymbol{\sigma}^{hardening} = \boldsymbol{s}^{hardening} = H\mathbf{e}, \tag{2}$$

where $\mathbf{e}$ is the total deviatoric strain and H is the hardening modulus.

2.1 Elastic part of the constitutive relations

The relation between stress and strain in the elastic domain is given by:

$$\boldsymbol{\sigma} = \boldsymbol{D} : \boldsymbol{\varepsilon}^e. \tag{3}$$

Here $\boldsymbol{\varepsilon}^e$ is the elastic strain and $\boldsymbol{D}$ is the fourth order elasticity tensor (fourth order elastic constitutive isotropic tensor) that is defined as follows:

$$\boldsymbol{D} = 2\mu \mathrm{I_s} + \lambda(\boldsymbol{I} \otimes \boldsymbol{I}), \tag{4}$$

where $\boldsymbol{I}$ is the second order identity tensor, $\mathrm{I_s}$ is a fourth order symmetric identity tensor and μ and λ are the Lame´s elastic material constants. The Cartesian components of $\mathrm{I_s}$ are given by:

$$\mathrm{I_s}_{\,ijkl} := \frac{1}{2}\big(\delta_{ik}\delta_{jl} + \delta_{il}\delta_{jk}\big). \tag{5}$$

In the case of separated deviatoric and volumetric stresses, the stress strain relations are given by:

$$\boldsymbol{s} = 2G\mathbf{e}^e \quad , \quad p = -K\boldsymbol{I}:\boldsymbol{\varepsilon}, \tag{6}$$

where $\boldsymbol{\varepsilon}$ is the total strain and $\mathbf{e}^e$ is the elastic deviatoric strain:

$$\mathbf{e}^e = dev[\boldsymbol{\varepsilon}^e] = \left[\mathrm{I_s} - \frac{1}{3}(\boldsymbol{I} \otimes \boldsymbol{I})\right] : \boldsymbol{\varepsilon}^e = \mathrm{I_d} : \boldsymbol{\varepsilon}^e \tag{7}$$

where $\mathrm{I_d}$ is the deviatoric projection tensor.

2.2 Yield criterion

The yield function for the Leonov model is defined as follows:

$$\phi := \overline{\sigma} - \overline{\sigma}_y \le 0, \tag{8}$$

where $\overline{\sigma}$ is the effective stress and $\overline{\sigma}_y$ is the uniaxial initial yield stress defined by:

$$\overline{\sigma} = \sqrt{\frac{3}{2}\boldsymbol{s} : \boldsymbol{s}}, \tag{9}$$

$$\overline{\sigma}_y = \frac{3}{\sqrt{3} + \mu}\left(\tau_0 \ln\left(2\sqrt{3}A_0\dot{\overline{e}}\right) + \mu p_0 + \frac{\Delta H\tau_0}{R\theta}\right), \tag{10}$$

where $\dot{\overline{e}}$ is the total equivalent strain rate, p_0 is the superimposed pressure of the analysis, R is the universal gas constant and θ is the absolute temperature. The other parameters $(\mu, \tau_0, \Delta H, A_0)$ in relation (10) are material properties.

2.3 Viscoplastic part of the constitutive relations

The rate of the viscoplastic strain is obtained by the following relation:

$$\dot{\boldsymbol{\varepsilon}}^{vp} = \frac{\boldsymbol{s}}{2\eta}, \tag{11}$$

where $\boldsymbol{\varepsilon}^{vp}$ is the viscoplastic strain; the second order tensor $\boldsymbol{s}$ is the deviatoric stress and η is the viscosity. The deviatoric stress is defined as:

$$\boldsymbol{s} := dev[\boldsymbol{\sigma}] = \boldsymbol{\sigma} + p\boldsymbol{I}, \tag{12}$$

where $\boldsymbol{I}$ is second order identity (unit tensor of order 2, $\boldsymbol{I}_{ij} = \delta_{ij}$) and p is the hydrostatic pressure defined by the following equation:

$$p = -\frac{1}{3} tr[\boldsymbol{\sigma}] = -\frac{1}{3}\boldsymbol{I} : \boldsymbol{\sigma}. \tag{13}$$

The viscoplastic flow rule in the Leonov model is characterized by the generalized Eyring equation. The viscosity is defined based on the Eyring flow relation and is defined as follows:

$$\eta = A_0 \exp\left[\frac{\Delta H}{R\theta} + \frac{\mu p}{\tau_0} - Q_\infty + Q_\infty \exp\left(\frac{-h}{Q_\infty}\sqrt{3}\overline{e}^{vp}\right)\right] \frac{\sqrt{\frac{1}{3}}\overline{\sigma}}{\sinh\left(\frac{\sqrt{\frac{1}{3}}\overline{\sigma}}{\tau_0}\right)}, \tag{14}$$

where $\overline{\sigma}$ is effective stress, $\overline{e}^{vp}$ is equivalent viscoplastic strain, p is hydrostatic pressure, R is the universal gas constant, θ is absolute temperature and the other parameters $(A_0, \Delta H, \mu, \tau_0, Q_\infty, h)$ are material properties.

3 NUMERICAL IMPLEMENTATION

Operator split algorithms are widely used for numerical integration of constitutive equations in the context of elasto-plasticity and elasto-viscoplasticity. Numerical implementation of constitutive models through finite element codes basically includes a state update procedure and the computation of the consistent tangent operator.

3.1 State update

Let us consider a typical time interval $[t_n, t_{n+1}]$. The set of variables $\{\boldsymbol{\sigma}_n, \boldsymbol{\varepsilon}_n^e, \boldsymbol{\varepsilon}_n^{vp}, \overline{e}_n^{vp}\}$ is known at time t_n and the main problem is to determine the same set $\{\boldsymbol{\sigma}_{n+1}, \boldsymbol{\varepsilon}_{n+1}^e, \boldsymbol{\varepsilon}_{n+1}^{vp}, \overline{e}_{n+1}^{vp}\}$ at time t_{n+1}. The operator split algorithm comprises an *Elastic predictor* and a *Return mapping* algorithm which are described in this subsection.

Elastic predictor
In this stage, we assume that the material behaves purely elastically. The elastic trial strain at time step t_{n+1} is assumed to be given by:

$$\boldsymbol{\varepsilon}_{n+1}^{e\ trial} = \boldsymbol{\varepsilon}_{n+1} = \boldsymbol{\varepsilon}_n^e + \Delta\boldsymbol{\varepsilon}. \tag{15}$$

The deviatoric part of the total strain is given by

$$\boldsymbol{\varepsilon}_{d\ n+1}^{e\ trial} = dev\left(\boldsymbol{\varepsilon}_{n+1}^{e\ trial}\right) = \left[\mathrm{I}_s - \frac{1}{3}(\boldsymbol{I} \otimes \boldsymbol{I})\right] : \boldsymbol{\varepsilon}_{n+1}^{e\ trial} = \mathrm{I}_d : \boldsymbol{\varepsilon}_{n+1}^{e\ trial}. \tag{16}$$

The trial deviatoric stress is given by:

$$\boldsymbol{s}_{n+1}^{trial} = 2G\boldsymbol{\varepsilon}_{d\ n+1}^{e\ trial}, \tag{17}$$

where G is shear modulus. The hydrostatic pressure is computed by:

$$p_{n+1}^{trial} = -K\varepsilon_{v\ n+1}^{e\ trial} \tag{18}$$

where K is bulk modulus and $\varepsilon_{v\ n+1}^{e\ trial}$ is

$$\varepsilon_{v\ n+1}^{e\ trial} = tr\left(\boldsymbol{\varepsilon}_{n+1}^{e\ trial}\right). \tag{19}$$

The trial accumulated viscoplastic strain is assumed to be frozen:

$$\overline{\varepsilon}_{n+1}^{vp\ trial} = \overline{\varepsilon}_n^{vp}. \tag{20}$$

After computing the aforementioned variables, checking the yield criterion determines whether the initial assumption based on being in the elastic domain is correct or not. If the yield function is satisfied, we are in the elastic domain, then we update the variables as

$$(\blacksquare)_{n+1} = (\blacksquare)_{n+1}^{trial} \tag{21}$$

If the yield criterion is not satisfied, we are in the viscoplastic domain which needs a return mapping scheme to update the state variables.

Return mapping
By manipulating the constitutive relations, two residual equations are obtained.

$$R_1\big(\bar{e}_{n+1}^{vp}, \bar{\sigma}_{n+1}\big) := \bar{e}_{n+1}^{vp} - \bar{e}_n^{vp} - \frac{\Delta t}{3\eta_{n+1}}\bar{\sigma}_{n+1} = 0 \tag{22}$$

$$R_2\big(\bar{e}_{n+1}^{vp}, \bar{\sigma}_{n+1}\big) := 3G\big(\bar{e}_{n+1}^{vp} - \bar{e}_n^{vp}\big) - \bar{\sigma}_{n+1}^{trial} + \bar{\sigma}_{n+1} = 0. \tag{23}$$

Where Δt is the time interval between two consecutive time steps. We will use the well-known Newton-Raphson iterative procedure to solve our system of residual equations. To do so, the following matrix representation is presented:

$$A\delta = B \tag{24}$$

where A is matrix of coefficients, δ is the array of unknowns and finally B is the array of constants. The components of the aforementioned matrix and arrays are represented in the following form:

$$\begin{bmatrix} \dfrac{\partial R_1\big(\bar{e}_{n+1}^{vp}, \bar{\sigma}_{n+1}\big)}{\partial \bar{e}_{n+1}^{vp}} & \dfrac{\partial R_1\big(\bar{e}_{n+1}^{vp}, \bar{\sigma}_{n+1}\big)}{\partial \bar{\sigma}_{n+1}} \\ \dfrac{\partial R_2\big(\bar{e}_{n+1}^{vp}, \bar{\sigma}_{n+1}\big)}{\partial \bar{e}_{n+1}^{vp}} & \dfrac{\partial R_2\big(\bar{e}_{n+1}^{vp}, \bar{\sigma}_{n+1}\big)}{\partial \bar{\sigma}_{n+1}} \end{bmatrix} \begin{bmatrix} \Delta\bar{e}_{n+1}^{vp} \\ \Delta\bar{\sigma}_{n+1} \end{bmatrix} = \begin{bmatrix} -R_1\big(\bar{e}_{n+1}^{vp}, \bar{\sigma}_{n+1}\big) \\ -R_2\big(\bar{e}_{n+1}^{vp}, \bar{\sigma}_{n+1}\big) \end{bmatrix}. \tag{25}$$

After computing the accumulated viscoplastic strain, $\bar{e}_{n+1}^{vp}$, and the effective stress, $\bar{\sigma}_{n+1}$, the following variables should be updated as follows:

$$\boldsymbol{\varepsilon}_{n+1}^{vp} = \boldsymbol{\varepsilon}_n^{vp} + \frac{3\big(\bar{e}_{n+1}^{vp} - \bar{e}_n^{vp}\big)\Delta t}{2\big(\bar{\sigma}_{n+1}\Delta t + 3\big(\bar{e}_{n+1}^{vp} - \bar{e}_n^{vp}\big)\Delta t G\big)}\boldsymbol{s}_{n+1}^{trial}, \tag{26}$$

$$\boldsymbol{s}_{n+1} = \frac{1}{1 + \dfrac{3G}{\bar{\sigma}_{n+1}}\big(\bar{e}_{n+1}^{vp} - \bar{e}_n^{vp}\big)}\boldsymbol{s}_{n+1}^{trial}, \tag{27}$$

$$\boldsymbol{\varepsilon}_{d\,n+1}^e = \frac{1}{1 + \dfrac{3G}{\bar{\sigma}_{n+1}}\big(\bar{e}_{n+1}^{vp} - \bar{e}_n^{vp}\big)}\frac{\boldsymbol{s}_{n+1}^{trial}}{2G}. \tag{28}$$

It must be emphasized here that after implementing the aforementioned relations for the state update, it was observed that due to the behavior of the first residual equation, convergence was not achieved in many problems. Therefore, in order to achieve convergence, the first residual equation was transformed into a logarithmic version. The new residual equation has the following form:

$$R_1\big(\bar{e}_{n+1}^{vp}, \bar{\sigma}_{n+1}\big) := \ln\big(\bar{e}_{n+1}^{vp} - \bar{e}_n^{vp}\big) - \ln(\Delta t) - \ln(\bar{\sigma}_{n+1}) + \ln(3) + \ln(\eta_{n+1}) = 0. \tag{29}$$

Using the new residual led us to a remarkable improvement in the convergence rate of the state update procedure.

3.2 Consistent tangent operator

In order to complete the numerical implementation of the compressible Leonov model within an implicit quasi-static integration scheme, we need to obtain the consistent tangent operator. In other words, since the full Newton-Raphson scheme will be used within an implicit finite element implementation of the Leonov model, the tangent stiffness matrix must be computed. The tangent stiffness matrix is assembled using the tangent operators which are derived by consistently linearizing the state update relations. The tangent operator has the following definition:

$$\mathbf{D} := \frac{d\boldsymbol{\sigma}_{n+1}}{d\boldsymbol{\varepsilon}_{n+1}}. \tag{30}$$

In the elastic domain, the tangent operator is the following:

$$\mathbf{D}_e = (2G + H)\left[\mathrm{I}_s - \frac{1}{3}(\boldsymbol{I} \otimes \boldsymbol{I})\right] + K(\boldsymbol{I} \otimes \boldsymbol{I}). \tag{31}$$

Exact linearization of the constitutive telations and performing some algebraic manipulations result in the following closed form relation for viscoplastic tangent operator.

$$\mathbf{D}_{vp} = \left(\frac{2G\eta_{n+1}}{\eta_{n+1} + \Delta t\, G} + H\right)\left[\mathrm{I}_s - \frac{1}{3}(\boldsymbol{I} \otimes \boldsymbol{I})\right] + K(\boldsymbol{I} \otimes \boldsymbol{I}) + \tag{32}$$

$$\frac{3G^2\Delta t}{\overline{\sigma}_{n+1}^{trial}\,\Omega\,\eta_{n+1}}\left[\frac{\Delta t C_1}{3\eta_{n+1}} + C_2\right]\boldsymbol{s}_{n+1} \otimes \boldsymbol{s}_{n+1} - \frac{GK\Delta t\,\mu}{\eta_{n+1}\Omega\tau_0}\,\boldsymbol{s}_{n+1} \otimes \boldsymbol{I}$$

Where

$$C_1 = -\sqrt{3}h\exp\left(\frac{-h}{Q_\infty}\sqrt{3}\overline{e}_{n+1}^{vp}\right), \tag{33}$$

$$C_2 = \left[\frac{\tau_0\sinh\left(\frac{\sqrt{\frac{1}{3}}\overline{\sigma}_{n+1}}{\tau_0}\right) - \sqrt{\frac{1}{3}}\overline{\sigma}_{n+1}\cosh\left(\frac{\sqrt{\frac{1}{3}}\overline{\sigma}_{n+1}}{\tau_0}\right)}{\tau_0\,\overline{\sigma}_{n+1}\sinh\left(\frac{\sqrt{\frac{1}{3}}\overline{\sigma}_{n+1}}{\tau_0}\right)}\right], \tag{34}$$

$$\Omega = 1 + \frac{\Delta t\, G}{\eta_{n+1}} + \frac{\Delta t\, \overline{\sigma}_{n+1}}{3\eta_{n+1}}(C_1 - 3GC_2). \tag{35}$$

4 NUMERICAL EXAMPLES

In order to check the performance of the numerical implementation, two examples are considered. In the single element compression test, it is shown that the implementation can capture the effects of superimposed hydrostatic pressure and strain rate on the deformation behavior. Furthermore, it is illustrated that by changing the first residual to a logarithmic

function, the convergence rate of the implementation is considerably improved. In addition to the single element test, a compression test is numerically performed on a standard specimen and the results are compared with available experimental results.

4.1 Single element test

A single element under compression is analyzed and true stress-strain curves are provided. A four node quadratic element with four Gauss points is used for the analysis. The dimensions of the element are (*1×1 mm*) and the displacement applied to the element is (*0.5 mm*). The material is assumed to be PET Copolyester 9921W (referred to as PET) and the material properties, taken from [12], are listed in Table 1.

Table 1: Material properties for PET

E(MPa)	v	ΔH	A_0	τ_0(MPa)	Q_∞	h	μ	R	H(MPa)
2211	0.4	2.3E+5	8.1E-26	0.9	27.3	205	0.047	8.3143	26

The test is performed at room temperature, under different hydrostatic pressures and with different strain rates. Figures 1 and 2 show the effects of strain rate and hydrostatic pressure on deformation behavior, respectively.
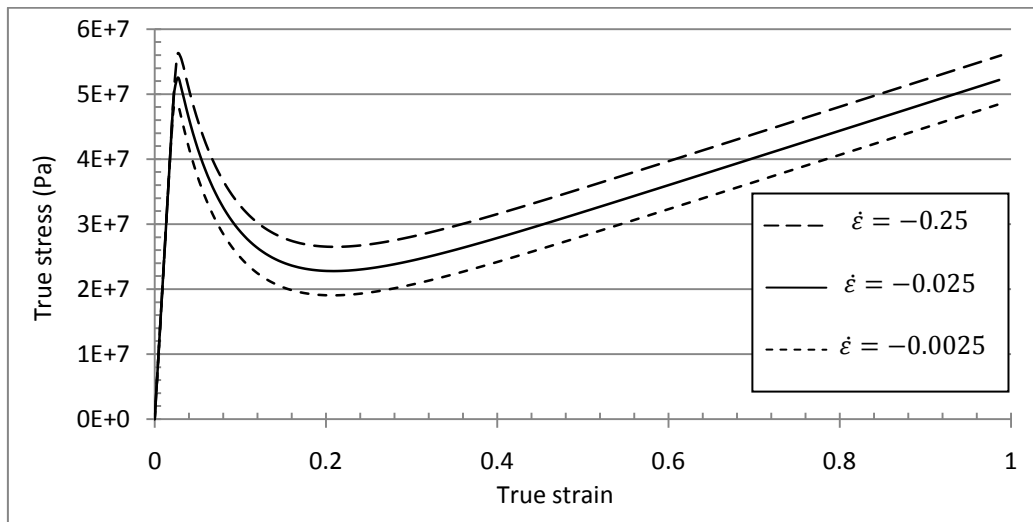

Figure 1: Stress strain curves for the single element compression test using PET at different strain rates under atmospheric condition ($P_0 = 0.1\ MPa$)

Table 2 shows the number of required iterations for a typical increment and corresponding residuals for the two different approaches. It can be clearly observed that the logarithmic transformation (indicated as the second approach) has been extremely effective to improve the convergence rate of the state update algorithm.

4.2 Standard specimen

The compression of a standard specimen is shown in Figure 3. In order to simulate the problem and due to symmetry , the simulation has been performed as a two-dimensional axisymmetric problem.
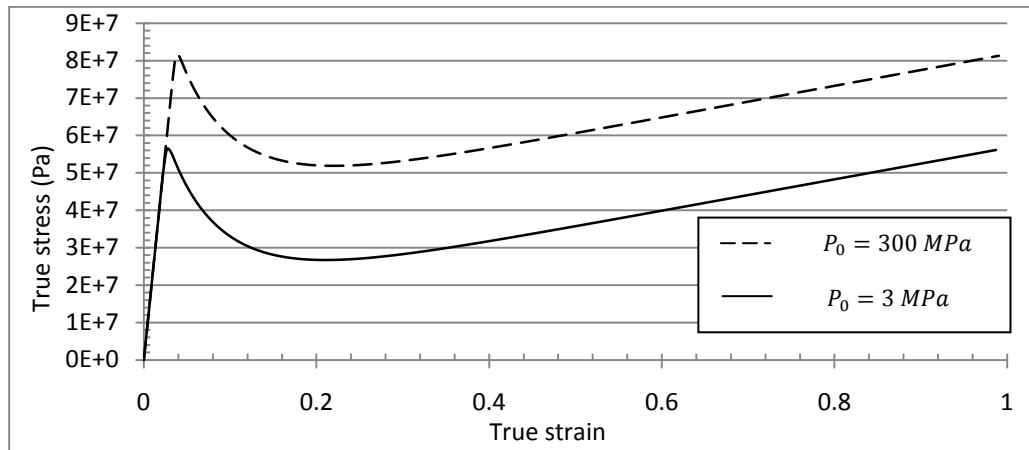

Figure 2: Stress strain curves for the single element compression test using PET at strain rate of $(\dot{\varepsilon} = -0.25)$ under different superimposed pressures

In fact, a rectangular with dimensions (*4mm× 2mm*) has been analyzed with 8 quadratic elements with dimensions (*1×1 mm*). The applied displacement is (*3 mm*). It must be noted that the hydrostatic pressure for this test is assumed to be $P_0 = 300\ MPa$, and the simulations have been performed assuming room temperature.

Figure 4 shows results obtained from both simulations and experiments for the compressed cylinder made from PET at the strain rate of $\dot{\varepsilon} = -0.25\ s^{-1}$. The experimental results are taken form [12].
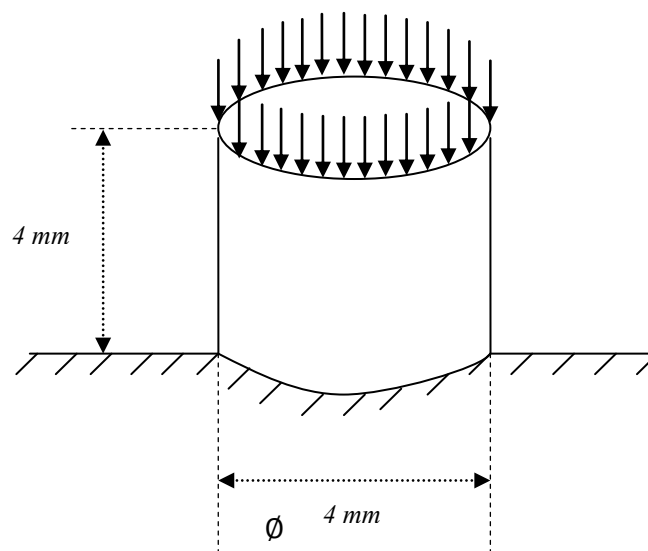

Figure 3: Schematic representation of the compressed cylinder (geometry, boundary conditions and loading)

A reasonable qualitative and quantitative agreement between numerical and experimental results can be observed.

Table 2: Convergence table for two approaches

Iteration no.	1st approach residual	2nd approach residual
1	0.636690	9.231974
2	2.435265E-2	0.135657
3	2.486794 E-2	7.634257E-4
4	2.540770 E-2	1.854449E-8
5	2.597371 E-2	
6	2.656790 E-2	
7	2.719243 E-2	
8	2.784967 E-2	
9	2.854220 E-2	
10	2.927289 E-2	
11	3.004483 E-2	
12	3.086112 E-2	
13	3.172435 E-2	
14	3.263460 E-2	
15	3.358365 E-2	
16	3.435756 E-2	
17	3.538555 E-2	
18	3.579642 E-2	
19	3.485924 E-2	
20	3.049617 E-2	
21	2.015115 E-2	
22	6.934124 E-3	
23	6.409727 E-4	
24	4.919388 E-6	
25	2.867187 E-10	

5 CONCLUSIONS

According to the results presented, it can be concluded that the numerical implementation is able to capture the effect of different parameters on the deformation behavior of polymeric based materials. Moreover, due to the considerable improvement on the convergence rate obtained by converting the first residual to a logarithmic function, it can be claimed that the transformation has been absolutely necessary. Finally, in view of the reasonable agreement

between simulations and experimental results, it seems that the Leonov model is able to predict the polymeric based materials behavior in compressive conditions adequately.
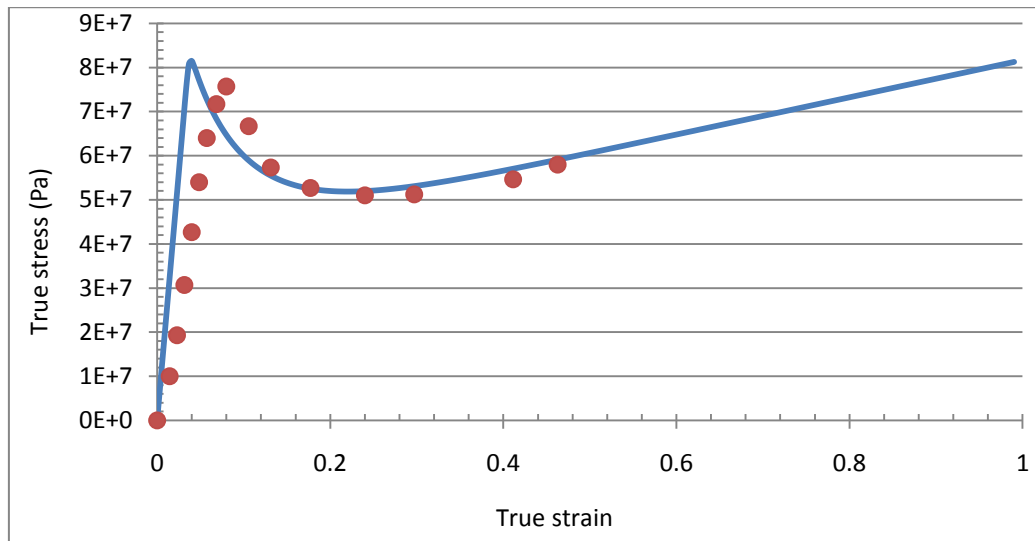

Figure 4: Stress strain curve for the compressed cylinder at the strain rate ($\dot{\varepsilon} = -0.25$). Solid line shows numerical simulations and circles show experimental results.

ACKNOWLEDGEMENTS

REFERENCES

[1] Baaijens, F.P.T. Calculation of residual stresses in injection molded products. *Rheol. Acta* (1991) **30**: 284–299.
[2] Boyce, M.C., Parks, D.M. and Argon, A.S. Large inelastic deformation of glassy polymers, Part I: Rate dependent constitutive model. *Mech. Mat* (1988) **7**: 15–33.
[3] De Souza Neto, E. A. A simple robust numerical integration algorithm for a power-law visco-plastic model under both high and low rate sensitivity. *Commun. Numer. Meth. Engng* (2004) **20**: 1-17.
[4] De Souza Neto, E. A., Peric, D., Owen, DRJ. *Computational methods for plasticity: Theory and applications*. Wiley (2008).
[5] Govaert, L., Timmermans, P., Brekelmans, W. The influence of intrinsic strain softening on strain localization in polycarbonate: modeling and experimental validation. *J. Engng. Mater. Tech* (2000) **122**: 177–185.
[6] Haward, R.N. and Thackray, G. The use of mathematical model to describe isothermal stress-strain curves in glassy polymers, *Proc. Roy. Soc. A* (1968) **302**: 453–472.
[7] Leonov, A. Non-equilibrium thermodynamics and rheology of viscoelastic polymer media. *Rheol. Acta* (1976) **15**: 85–98.

[8] Masud, A. and Chudnovsky A. A constitutive model of cold drawing in polycarbonates. *Int. J. Plasticity* (1999) **15**: 1139-1157.

[9] Tervoort, T., Smit, R., Brekelmans, W., Govaert, L. A constitutive equation for the elasto-viscoplastic deformation of glassy polymers. *Mech. Time Dep. Mater* (1998) **1**: 269–291.

[10] Tervoort, T. Constitutive Modelling of Polymer Glasses: Finite, Nonlinear Viscoelastic Behaviour of Polycarbonate. *Ph.D. thesis*, Eindhoven University of Technology, Eindhoven, The Netherlands (1996).

[11] Timmermans, P.H.M. Evaluation of a constitutive model for solid polymeric materials: model selection and parameter quantification. *Ph.D. thesis*, Eindhoven University of Technology, Eindhoven, The Netherlands (1997).

[12] Van der Aa. Michiel A.H. Wall ironing of polymer coated sheet metal. *PhD. thesis*, Eindhoven University of Technology, Eindhoven, The Netherlands (1999).

[13] Wu, P., van der Giessen, E. Analysis of shear band propagation in amorphous glassy polymers. *Int. J. Solids Structures* (1994) **31**: 1493–1517